NANO LETTERS

pubs.acs.org/NanoLett

Electrospun Ultralong Hierarchical Vanadium Oxide Nanowires with High Performance for Lithium Ion Batteries

Liqiang Mai,*[,†,‡] Lin Xu,[†] Chunhua Han,[†] Xu Xu,[†] Yanzhu Luo,[†] Shiyong Zhao,[†] and Yunlong Zhao[†]

[†]State Key Laboratory of Advanced Technology for Materials Synthesis and Processing, School of Materials Science and Engineering, Wuhan University of Technology, Wuhan 430070, China, and [‡]Department of Chemistry and Chemical Biology, Harvard University, Cambridge, Massachusetts 02138, United States

ABSTRACT Ultralong hierarchical vanadium oxide nanowires with diameter of 100−200 nm and length up to several millimeters were synthesized using the low-cost starting materials by electrospinning combined with annealing. The hierarchical nanowires were constructed from attached vanadium oxide nanorods of diameter around 50 nm and length of 100 nm. The initial and 50th discharge capacities of the ultralong hierarchical vanadium oxide nanowire cathodes are up to 390 and 201 mAh/g when the lithium ion battery cycled between 1.75 and 4.0 V. When the battery was cycled between 2.0 and 4.0 V, the initial and 50th discharge capacities of the nanowire cathodes are 275 and 187 mAh/g. Compared with self-aggregated short nanorods synthesized by hydrothermal method, the ultralong hierarchical vanadium oxide nanowires exhibit much higher capacity. This is due to the fact that self-aggregation of the unique nanorod-in-nanowire structures have been greatly reduced because of the attachment of nanorods in the ultralong nanowires, which can keep the effective contact areas of active materials, conductive additives, and electrolyte large and fully realize the advantage of nanomaterial-based cathodes. This demonstrates that ultralong hierarchical vanadium oxide nanowire is one of the most favorable nanostructures as cathodes for improving cycling performance of lithium ion batteries.

KEYWORDS Electrospinning, annealing, V_2O_5, nanowires, cathode, electrochemistry

Functional nanostructured architectures assembled from nanowires, nanobelts, nanotubes, or other nanocrystals as the building blocks will offer tremendous impact in many areas, such as nanoscale solar cells, nanogenerators, molecular electronics, and biological materials.[1−8] To serve as cathodes or anodes for lithium ion batteries, nanostructured active materials have a short Li-ion insertion/extraction distance, facile strain relaxation upon electrochemical cycling, and very large surface to volume ratio to contact with the electrolyte, which can improve the capacity and cycle life of lithium ion batteries.[9−16] However, in the ordinary batteries, owing to the high surface energy, nanomaterials are often self-aggregated, which reduces the effective contact areas of active materials, conductive additives, and electrolyte. How to keep the effective contact areas large and fully realize the advantage of active materials at nanometer scale is still a challenge and of great importance. Hierarchical nanostructured materials such as hollow nanospheres, porous nanostructures, nanotubes, nanowire-on-nanowire structures, and kinked nanowires, etc., can ensure the surface remains uncovered to keep the effective contact areas large even if a small amount of inevitable self-aggregation occurs.[17−21] Moreover, if one dimension of the nanocrystallites is up to a few hundred micrometers or even at millimeter scale, such as ultralong nanowires or nanobelts, self-aggregation of the nanomaterials can be effectively prevented. Therefore, to some extent, an ultralong hierarchical nanowire is one of the most favorable structures as cathode/anode materials for high-performance lithium ion batteries.

As a kind of promising cathode material, long vanadium oxide nanowires/nanobelts can be synthesized by hydrothermal reaction,[22,23] vapor transport,[24] and electrospinning.[25−28] It is particularly worth noting that electrospinning has been widely used as a convenient and versatile method for preparing ultralong hierarchical nanowires with controllable lengths, diameters, compositions, and complex architectures. There has been much interest in electrospinning and/or electrochemistry of vanadium oxide nanowires/nanorods because nanostructured vanadium/molybdenum oxides with a typical layed structure have the potential to offer high capacities for lithium ion batteries.[29−40] For example, V_2O_5 nanorods on TiO_2 nanowires, spiral-like V_2O_5 nanowires have been fabricated by electrospinning and annealing.[25,26] V_2O_5 nanocrystallites synthesized by electrospinning combined with hydrothermal treatment followed by annealing exhibit a high capacity of 350 mAh/g and high Columbic efficiency.[27]

In the previous work, we found that hierarchical $FeSe_2$ nanoflowers composed of uniform nanoplates exhibited high discharge capacity of ca. 431 mAh/g even if inevitable self-aggregation occurred.[41] Here, we report a novel hierar-

* Address correspondence to mlq@cmliris.harvard.edu.
Received for review: 09/21/2010
Published on Web: 10/18/2010

DOI: 10.1021/nl103343w | *Nano Lett.* **2010,** *10,* 4750–4755

chical nanostructure, which is ultralong vanadium oxide nanowires constructed from attached single-crystalline vanadium oxide nanorods. Compared with previous studies on electrospinning of vanadium oxide nanowires by using expensive organic vanadium oxide isopropoxide as the raw materials, we successfully synthesized vanadium oxide nanowires via electrospinning by using inorganic ammonium metavanadate as precursor, which is cost-saving and more suitable for industrial production of lithium batteries. Moreover, the as-prepared ultralong hierarchical vanadium oxide nanowires were found to offer high charge/discharge capacities and improved cycling stability.

Poly(vinyl alcohol) (PVA) ($M_w = 80000$) and ammonium metavanadate (NH_4VO_3) were commercially available and used as received. Twenty milliliters of aqueous PVA solution with a concentration of 10 wt % was first prepared by dissolving PVA powder in deionized water and heating at 80 °C with vigorous stirring for 5 h, and 0.5 g of NH_4VO_3 was then added to the above PVA solution. After the mixture was stirred at 70 °C for 3 h, a viscous light-yellow clear solution of ammonium metavanadate/PVA was obtained. The precursor solution was then delivered into a metallic needle at a constant flow rate of 1.0 mL/h by a computer-controlled syringe pump. The metallic needle was connected to a high-voltage power supply, and a piece of grounded aluminum foil was placed 20 cm below the tip of the needle. As a high voltage of 20 kV was applied, the precursor solution jet accelerated toward the aluminum foil, leading to the formation of NH_4VO_3/PVA composite nanowires accompanied by rapid evaporation of solvent. The composite nanowires were then annealed at 480 °C in air for 3 h to obtain ultralong hierarchical vanadium oxide nanowires.

An X-ray diffraction (XRD) measurement was performed using a D/MAX-III X-ray diffractometer with graphite-monochromatized Cu Kα radiation. For XRD measurement, the nanowire mats were separated from Al substrate and then slightly pressed on a glass slide to form a dense film. Fourier-transformed infrared (FTIR) absorption spectra were recorded using the 60-SXB IR spectrometer. Field emission scanning electron microscopy (FESEM) images were collected with a Hitachi S-4800 at an acceleration voltage of 20 kV. Transmission electron microscopy (TEM) and high-resolution transmission electron microscopy (HRTEM) were recorded by using a JEOL JEM-2010 FEF microscope. Thermogravimetry/differential scanning calorimetry (TG/DSC) was performed using a Netzsch STA 449C simultaneous thermal analyzer at a heating rate of 10 °C/min in air. The electrochemical properties were studied with a multichannel battery testing system (Neware BTS-5 V/5 mA). Batteries were fabricated using a lithium pellet as the anode, 1 M solution of $LiPF_6$ in ethylene carbon (EC)/dimethyl carbonate (DMC) as electrolyte, and a pellet made of the nanowires, acetylene black, and PTFE (polytetrafluoroethylene) in a 70:25:5 weight ratio as the cathode. Galvanostatic charge/discharge tests were performed over the potential region of 2.0−4.0 and 1.75−4.0 V, respectively, at a current density of 30 mA/g and temperature of 25 °C.

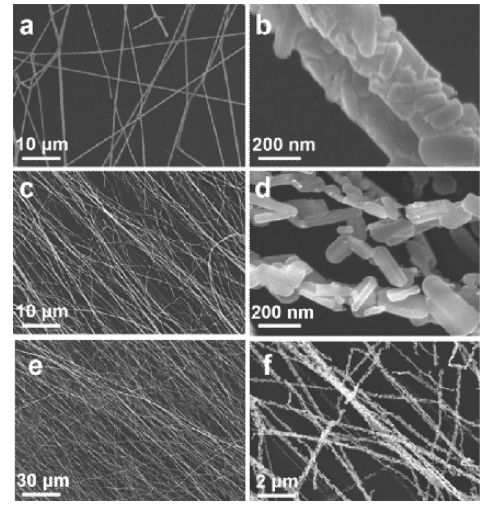

FIGURE 1. (a, b) FESEM images of electrospun NH_4VO_3/PVA composite nanowires. (c−f) FESEM images of the ultralong hierarchical vanadium oxide nanowires after annealing.

Panels a and b of Figure 1 show the low and high magnification FESEM images of the as-electrospun ultralong NH_4VO_3/PVA composite nanowires at the 1:4 weight ratio of NH_4VO_3 and PVA for the starting materials. As observed, the length of the nanowires can even reach the millimeter or centimeter grade. The collected nanowires aligned in random orientation because of the bending instability associated with the spinning jet. Each individual nanowire was uniform in cross section, with an average diameter of 200−250 nm. Interestingly, short nanorods of diameter about 50 nm and length of 100 nm were grown on the surface of the nanowires, which was quite different from that in the literature on electrospinning of vanadium oxide nanowires from vanadium oxide isopropoxide.[26] The nanorod-in-nanowire structures could be accounted for the limited solubility of NH_4VO_3 in water at room temperature. The electrospun composite nanowires were then annealed at 480 °C in air for 3 h to obtain vanadium oxide nanowires. After annealing, the nanowires could remain long as the continuous structures, while the diameter decreased to 100−200 nm (Figure 1c−f). Notably, it was found that the ultralong vanadium oxide nanowires were constructed from attached nanorods of diameter around 50 nm and length of 100 nm. The size reduction of the nanowires was probably caused by the loss of PVA from the nanowires and thermal decomposition of NH_4VO_3. When the weight ratio of NH_4VO_3 and PVA decreased to 1:7 for the starting materials, the ultralong and continuous vanadium oxide nanowires could still be formed (Figure S1 in the Supporting Information). This indicates that the low-cost NH_4VO_3 which we used in this work can be considered as a kind of excellent precursor for electrospinning of vanadium oxide nanowires.

XRD patterns show that the as-electrospun composite nanowires were composed of NH_4VO_3 and PVA (Figure 2a).

DOI: 10.1021/nl103343w | *Nano Lett.* **2010,** *10,* 4750−4755

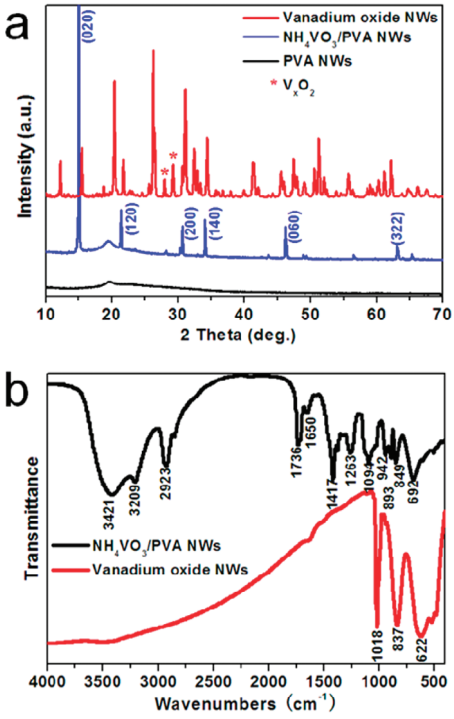

FIGURE 2. (a) XRD patterns of electrospun PVA nanowires, NH_4VO_3/PVA nanowires, and the ultralong hierarchical vanadium oxide nanowires after annealing. (b) FTIR spectra of electrospun NH_4VO_3/PVA composite nanowires and the ultralong hierarchical vanadium oxide nanowires after annealing.

Surprisingly, the intensity of (020) peak of NH_4VO_3 nanorods on the nanowires was extremely strong compared with other diffraction peaks, showing a well-defined (020) crystal plane orientation. XRD patterns of the nanowires after annealing can be indexed to orthorhombic V_2O_5, including a small amount of V_xO_2. FTIR spectroscopy was applied to further investigate the structural change in bonding related to the electrospun nanowires before and after annealing (Figure 2b). For NH_4VO_3/PVA composite nanowires, the strong bands observed between 500 and 2000 cm^{-1} can be assigned to bending and stretching frequencies of PVA. The band at 3209 cm^{-1} is assigned to vibrations of NH_4^+, and the band at 2923 cm^{-1} is assigned to vibrations of $-CH_2-$. The bands at 3421 and 1650 cm^{-1} are assigned to stretching and bending frequencies of adsorbed water. After annealing, the bands assigned to PVA disappeared; instead, well-defined features are observed due to vanadium oxide. The evidence for the structural determination of orthorhombic V_2O_5 crystals is the peak position of the vanadyl (V═O) mode located at 1018 cm^{-1}. The other bands at 837 and 622 cm^{-1} are assigned to the vibrations of V—O—V and O—$(V)_3$, respectively. TG/DSC analysis can also confirm that the complete formation of pure inorganic oxide occurred above 480 °C (Figure S2 in the Supporting Information).

TEM and HRTEM investigations were conducted to further analyze the secondary structures of the ultralong hierarchical vanadium oxide nanowires, as shown in Figure 3. Notably, the nanorods were tightly attached with each other

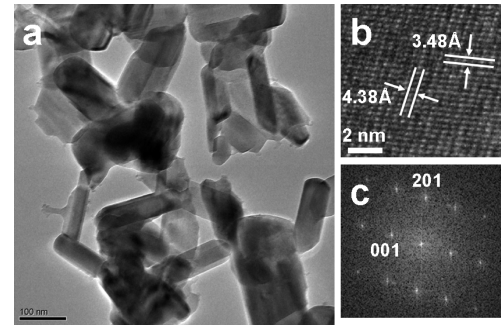

FIGURE 3. (a) TEM image of the ultralong hierarchical vanadium oxide nanowires after annealing. (b) HRTEM image and (c) FFT patterns of a single nanorod on the hierarchical vanadium oxide nanowires.

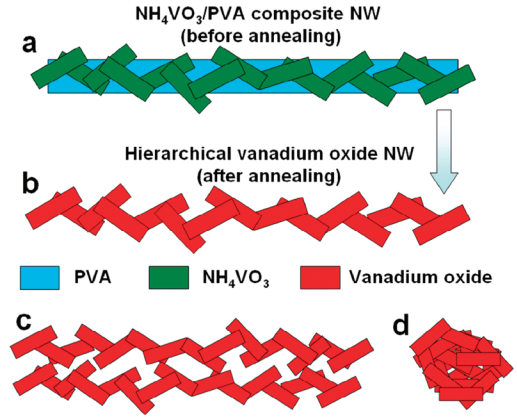

FIGURE 4. (a, b) Schematic illustration of formation of the ultralong hierarchical vanadium oxide nanowires during annealing. (c) Side view of two ultralong hierarchical vanadium oxide nanowires near each other. (d) Self-aggregation of short vanadium oxide nanorods.

to construct the nanowires (Figure 3a and Figure S3 in the Supporting Information). Figure 3b shows lattice fringes of a nanorod with regular spacing of 4.38 and 3.48 Å, which are consistent with the interplanar distance of (001) and (201) planes of V_2O_5. The well-resolved fringes confirm the local single crystallinity of the V_2O_5 nanorods, which is in accordance with the corresponding fast Fourier transformation (FFT) patterns shown in Figure 3c.

The following possible formation mechanism for the ultralong hierarchical vanadium oxide nanowires is suggested: In the process of preparing NH_4VO_3/PVA solution before electrospinning, NH_4VO_3 and PVA were completely dissolved in hot water to form a clear viscous sol. When the precursor solution jet accelerated toward the grounded aluminum foil, NH_4VO_3 crystals began to grow accompanied by rapid evaporation of solvent. Meanwhile, the PVA nanowire played the role of a template for the oriented growth of attached NH_4VO_3 nanorods, which resulted in the formation of ultralong hierarchical NH_4VO_3/PVA composite nanowires, as illustrated in Figure 4a. This is in accordance with the FESEM images and XRD pattern of the electrospun nanowires (Figure 1b and Figure 2a). During annealing,

DOI: 10.1021/nl103343w | *Nano Lett.* **2010,** *10,* 4750–4755

NH_4VO_3 and PVA decomposed, while the attached nanorods could keep the morphologies when the phase transition occurred. Finally, the ultralong hierarchical vanadium oxide nanowires made up of attached nanorods were formed, as illustrated in Figure 4b, which can be confirmed by FESEM images of the annealed nanowires in Figure 1c,d. Figure 4c is the schematic illustration of two ultralong hierarchical vanadium oxide nanowires near each other. It was shown that the self-aggregation of nanorods had been greatly reduced because of the attachment of nanorods in the nanowires. For comparison, self-aggregation of the common short nanorods was illustrated in Figure 4d. The well-dispersed hierarchical nanowires will have potential applications in electrochemistry due to available high surface areas.

Figure 5a shows the potential versus capacity curves of the first and 10th cycles for the ultralong hierarchical vanadium oxide nanowires cycled between 2.0 and 4.0 V. The first discharge and chagre capacities are both 275 mAh/g, showing no capacity loss in the first cycle. The typical plateaus corresponding to the phase transitions of cryatalline V_2O_5 were obviously observed. However, two additional plateaus at 2.8 and 2.5 V are not like the characteristic of V_2O_5 cathode, which is probably due to other electrochemically active vanadium oxides with low valence state of vanadium,[29] that is, V_xO_2, as indicated in Figure 2a. After 10 cycles, the multistep charge/discharge behavior still occurred, which means irreversible ω-$Li_3V_2O_5$ were not formed.[29] When the battery was cycled between 1.75 and 4.0 V, The first discharge and charge capacities are up to 390 and 361 mAh/g, respectively (Figure 5b). However, during the 10th cycle, the multistep discharge behavior disappeared, which was due to the irreversible formation of ω-$Li_3V_2O_5$ when the electrochemical intercalation of lithium in V_2O_5 occurred at a voltage smaller than 1.9 V.[42,43] After 50 cycles, the discharge capacities can reach 201 mAh/g at 1.75−4.0 V and 187 mAh/g at 2.0−4.0 V (Figure 5c), exhibiting the greatly improved performance for lithium batteries. We found that the cycling efficiency of the battery cycled at 2.0−4.0 V was higher and more stable than that at 1.75−4.0 V, which was attributed to irreversible phase transition at 1.9 V.

The high performance of our batteries is attributed to several reasons. We deduce that self-aggregation of the ultralong hierarchical vanadium oxide nanowires can be effectively prevented, which keeps the surface area large to fully realize the advantage of nanostructured materials. Furthermore, after annealing at 480 °C, the vanadium oxide nanorods of high crystallinity in the nanowires make the active materials stable during cycling. Similar results were reported by Whittingham's group that cycling stability of V_2O_5 nanorods is improved by annealing.[27,29] Compared with other vanadium oxide nanorods by combining electrospinning with hydrothermal treatment or annealing,[27,29] our ultralong hierarchical vanadium oxide nanowires have higher specific capacity and better cycling capability. Meanwhile, we have prepared vanadium oxide nanorods with lengths of about 1−2 μm by the hydrothermal method. It was found that these short nanorods were easily self-aggregated together, which exhibited a low discharge capacity of 110−130 mAh/g (Figure S4 in the Supporting Information). Therefore, ultralong hierarchical nanowire constructed from attached nanorods/nanoparticles as the building blocks may be a special structure that is superior to nanoparticles or short nanorods in lithium ion battery applications.

In summary, using low-cost NH_4VO_3 as the starting materials, we have developed a cost-saving method to

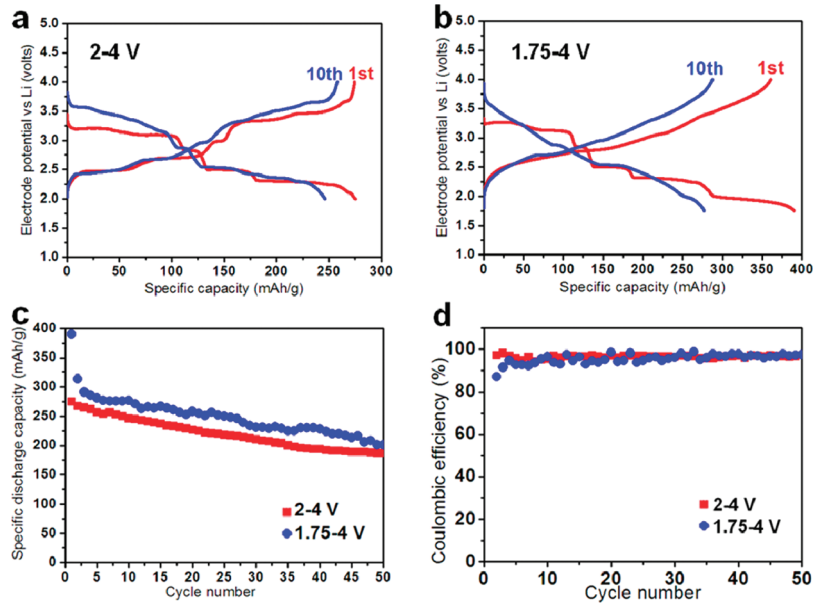

FIGURE 5. (a, b) Charge/discharge curves of hierarchical vanadium oxide nanowires at voltages of 2−4 and 1.75−4 V, respectively. (c, d) Capacity vs cycle number, and Coulombic efficiency vs cycle number of the ultralong hierarchical vanadium oxide nanowires.

DOI: 10.1021/nl103343w | *Nano Lett.* **2010,** *10,* 4750–4755

prepare ultralong hierarchical vanadium oxide nanowires constructed from attached vanadium oxide nanorods. The growth of NH_4VO_3 nanorods on the surface of electrospun NH_4VO_3/PVA composite nanowires before annealing is critical for the formation of hierarchical vanadium oxide nanowires. This novel nanostructure exhibits a high performance for lithium ion batteries, providing a high discharge capacity of 390 mAh/g and improved cycling stability, which results from reduced self-aggregation of the nanomaterials. The nanorod-in-nanowire described in this paper is a unique structure that will probably have potential applications in chemical power sources, sensors, and other nanodevices.

Acknowledgment. This work was partially supported by the National Nature Science Foundation of China (50702039, 51072153), the Research Fund for the Doctoral Program of Higher Education (20070497012), the Fundamental Research Funds for the Central Universities (2010-II-016), and Scientific Research Foundation for Returned Scholars, Ministry of Education of China (2008−890). We express our thanks to Professor C. M. Lieber of Harvard University for his strong support and stimulating discussion.

Supporting Information Available. FESEM images of the other ultralong vanadium oxide nanowires, TG-DSC curves of the samples, HRTEM images of two attached nanorods in the samples, and FESEM images and discharge capacity of short self-aggregated vanadium oxide nanorods for comprision. This material is available free of charge via the Internet at http://pubs.acs.org.

REFERENCES AND NOTES

(1) Tian, B.; Zheng, X.; Kempa, T. J.; Fang, Y.; Yu, N.; Yu, G.; Huang, J.; Lieber, C. M. Coaxial Silicon Nanowires as Solar Cells and Nanoelectronic Power Sources. *Nature* **2007**, *449*, 885–890.

(2) Javey, A.; Nam, S. W.; Friedman, R. S.; Yan, H.; Lieber, C. M. Layer-by-Layer Assembly of Nanowires for Three-Dimensional, Multifunctional Electronics. *Nano Lett.* **2007**, *7*, 773–777.

(3) Xu, S.; Qin, Y.; Xu, C.; Wei, Y.; Yang, R.; Wang, Z. L. Self-Powered Nanowire Devices. *Nat. Nanotechnol.* **2010**, *5*, 366–373.

(4) Yang, R.; Qin, Y.; Dai, L.; Wang, Z. L. Power Generation with Laterally Packaged Piezoelectric Fine Wires. *Nat. Nanotechnol.* **2009**, *4*, 34–39.

(5) Qian, M.; Reber, A. C.; Ugrinov, A.; Chaki, N. K.; Mandal, S.; Saavedra, H. M.; Khanna, S. N.; Sen, A.; Weiss, P. S. Cluster-Assembled Materials: Toward Nanomaterials with Precise Control over Properties. *ACS Nano* **2010**, *4*, 235–240.

(6) Briseno, A. L.; Holcombe, T. W.; Boukai, A. I.; Garnett, E. C.; Shelton, S. W.; Fréchet, J. M. J.; Yang, P. Oligo- and Polythiophene/ZnO Hybrid Nanowire Solar Cells. *Nano Lett.* **2010**, *10*, 334–340.

(7) Garnett, E.; Yang, P. Light Trapping in Silicon Nanowire Solar Cells. *Nano Lett.* **2010**, *10*, 1082–1087.

(8) Lu, Z.; Ye, M.; Li, N.; Zhong, W.; Yin, Y. Self-Assembled TiO_2 Nanocrystal Clusters for Selective Enrichment of Intact Phosphorylated Proteins. *Angew. Chem., Int. Ed.* **2010**, *49*, 1862–1866.

(9) Chan, C. K.; Peng, H.; Liu, G.; Mcilwrath, K.; Zhang, X. F.; Huggins, R. A.; Cui, Y. High-Performance Lithium Battery Anodes Using Silicon Nanowires. *Nat. Nanotechnol.* **2008**, *3*, 31–35.

(10) Zhai, T.; Liu, H.; Li, H.; Fang, X.; Liao, M.; Li, L.; Zhou, H.; Koide, Y.; Bando, Y.; Golberg, D. Centimeter-Long V_2O_5 Nanowires: From Synthesis to Field-Emission, Electrochemical, Electrical Transport, and Photoconductive Properties. *Adv. Mater.* **2010**, *22*, 2547–2552.

(11) Chou, S. L.; Wang, J. Z.; Sun, J. Z.; Wexler, D.; Forsyth, M.; Liu, H. K.; Macfarlane, D. R.; Dou, S. X. High Capacity, Safety, and Enhanced Cyclability of Lithium Metal Battery Using a V_2O_5 Nanomaterial Cathode and Room Temperature Ionic Liquid Electrolyte. *Chem. Mater.* **2008**, *20*, 7044–7051.

(12) Liu, J.; Xia, H.; Xue, D.; Lu, L. Double-Shelled Nanocapsules of V_2O_5-Based Composites as High-Performance Anode and Cathode Materials for Li Ion Batteries. *J. Am. Chem. Soc.* **2009**, *131*, 12086–12087.

(13) Mai, L.; Dong, Y.; Xu, L.; Han, C. Single Nanowire Electrochemical Devices. *Nano Lett.* **2010**, *10*, 4273–4278.

(14) Gao, S.; Chen, Z.; Wei, M.; Wei, K.; Zhou, H. Single Crystal Nanobelts of $V_3O_7 \cdot H_2O$: A Lithium Intercalation Host with a Large Capacity. *Electrochim. Acta* **2009**, *54*, 1115–1118.

(15) Reddy, C. V. S.; Wei, J.; Quan-Yao, Z.; Zhi-Rong, D.; Wen, C.; Mho, S.; Kalluru, R. R. Cathodic Performance of (V_2O_5 + PEG) Nanobelts for Li Ion Rechargeable Battery. *J. Power Sources* **2007**, *166*, 244–249.

(16) Semenenko, D. A.; Itkis, D. M.; Pomerantseva, E. A.; Goodilin, E. A.; Kulova, T. L.; Skundin, A. M.; Tretyakov, Y. D. $Li_xV_2O_5$ Nanobelts for High Capacity Lithium-Ion Battery Cathodes. *Electrochem. Commun.* **2010**, *12*, 1154–1157.

(17) Brezesinski, T.; Wang, J.; Tolbert, S. H.; Dunn, B. Ordered Mesoporous α-MoO_3 with Iso-oriented Nanocrystalline Walls for Thin-Film Pseudocapacitors. *Nat. Mater.* **2010**, *9*, 146–151.

(18) Tian, B.; Xie, P.; Kempa, T. J.; Bell, D. C.; Lieber, C. M. Single-Crystalline Kinked Semiconductor Nanowire Superstructures. *Nat. Nanotechnol.* **2009**, *4*, 824–829.

(19) Ge, J.; Hu, Y.; Biasini, M.; Beyermann, W. P.; Yin, Y. Superparamagnetic Magnetite Colloidal Nanocrystal Clusters. *Angew. Chem., Int. Ed.* **2007**, *46*, 4342–4345.

(20) Zhang, Q.; Wang, W.; Goebl, J.; Yin, Y. Self-Templated Synthesis of Hollow Nanostructures. *Nano Today* **2009**, *4*, 494–507.

(21) Ge, J.; Zhang, Q.; Zhang, T.; Yin, Y. Core-Satellite Nanocomposite Catalysts Protected by a Porous Silica Shell: Controllable Reactivity, High Stability, and Magnetic Recyclability. *Angew. Chem., Int. Ed.* **2008**, *47*, 8924–8928.

(22) Liu, J.; Wang, X.; Peng, Q.; Li, Y. Vanadium Pentoxide Nanobelts: Highly Selective and Stable Ethanol Sensor Materials. *Adv. Mater.* **2005**, *17*, 764–767.

(23) Liu, J.; Wang, X.; Peng, Q.; Li, Y. Preparation and Gas Sensing Properties of Vanadium Oxide Nanobelts Coated with Semiconductor Oxides. *Sens. Actuators, B* **2006**, *115*, 481–487.

(24) Wu, M. C.; Lee, C. S. Field emission of vertically aligned V_2O_5 nanowires on an ITO surface prepared with gaseous transport. *J. Solid State Electrochem.* **2009**, *182*, 2285–2289.

(25) Ostermann, R.; Li, D.; Yin, Y.; McCann, J. T.; Xia, Y. V_2O_5 Nanorods on TiO_2 Nanofibers: A New Class of Hierarchical Nanostructures Enabled by Electrospinning and Calcination. *Nano Lett.* **2006**, *6*, 1297–1302.

(26) Viswanathamurthi, P.; Bhattarai, N.; Kim, H. K.; Lee, D. R. Vanadium Pentoxide Nanofibers by Electrospinning. *Scr. Mater.* **2003**, *49*, 577–581.

(27) Ban, C.; Chernova, N. A.; Whittingham, M. S. Electrospun Nano-Vanadium Pentoxide Cathode. *Electrochem. Commun.* **2009**, *11*, 522–525.

(28) Ban, C.; Whittingham, M. S. Nanoscale Single-Crystal Vanadium Oxides with Layered Structure by Electrospinning and Hydrothermal Methods. *Solid State Ionics* **2008**, *179*, 1721–1724.

(29) Chernova, N. A.; Roppolo, M.; Dillonb, A. C.; Whittingham, M. S. Layered Vanadium and Molybdenum Oxides: Batteries and Electrochromics. *J. Mater. Chem.* **2009**, *10*, 2526–2552.

(30) Chan, C. K.; Peng, H.; Twesten, R. D.; Jarausch, K.; Zhang, X. F.; Cui, Y. Fast, Completely Reversible Li Insertion in Vanadium Pentoxide Nanoribbons. *Nano Lett.* **2007**, *7*, 490–495.

(31) Mai, L. Q.; Chen, W.; Xu, Q.; Peng, J. F.; Zhu, Q. Y. Mo Doped Vanadium Oxide Nanotubes: Microstructure and Electrochemistry. *Chem. Phys. Lett.* **2003**, *382*, 307–312.

(32) Chen, W.; Mai, L. Q.; Qi, Y. Y.; Dai, Y. One-Dimensional Nanomaterials of Vanadium and Molybdenum Oxides. *J. Phys. Chem. Solids* **2006**, *67*, 896–902.

DOI: 10.1021/nl103343w | *Nano Lett.* **2010,** *10,* 4750–4755

(33) Mai, L. Q.; Gu, Y.; Han, C. H.; Hu, B.; Chen, W.; Zhang, P. C.; Xu, L.; Guo, W. L.; Dai, Y. Orientated Langmuir-Blodgett Assembly of VO_2 Nanowires. *Nano Lett.* **2009**, *9*, 826–830.
(34) Mai, L. Q.; Guo, W. L.; Hu, B.; Jin, W.; Chen, W. Fabrication and Properties of VO_x-Based Nanorods. *J. Phys. Chem. C* **2008**, *112*, 423–429.
(35) Cao, J.; Musfeldt, J. L.; Mazumdar, S.; Chernova, N. A.; Whittingham, M. S. Pinned Low-Energy Electronic Excitation in Metal-Exchanged Vanadium Oxide Nanoscrolls. *Nano Lett.* **2007**, *7*, 2351–2355.
(36) Whitingham, M. S.; Song, Y.; Lutta, S.; Zavalij, P. Y.; Chernova, N. Some Transition Metal (oxy)phosphates and Vanadium Oxides for Lithium Batteries. *J. Mater. Chem.* **2005**, *15*, 3362–3379.
(37) Mai, L. Q.; Hu, B.; Chen, W.; Qi, Y. Y.; Lao, C. S.; Yang, R. S.; Wang, Z. L. Lithiated MoO_3 Nanobelts with Greatly Improved Performance for Lithium Battery. *Adv. Mater.* **2007**, *19*, 3712–3716.
(38) Mai, L. Q.; Lao, C. S.; Hu, B.; Zhou, J.; Qi, Y. Y.; Chen, W.; Gu, E. D.; Wang, Z. L. Synthesis and Electrical Transport of Single Crystal $NH_4V_3O_8$ Nanobelts. *J. Phys. Chem. B* **2006**, *110*, 18138–18141.
(39) Mai, L. Q.; Hu, B.; Hu, T.; Chen, W.; Gu, E. D. Electrical Property of Mo-doped VO_2 Nanowire Array Film by Melting-quenching Sol-gel Method. *J. Phys. Chem. B* **2006**, *110*, 19083–19086.
(40) Hu, B.; Mai, L. Q.; Chen, W.; Yang, F. From MoO_3 Nanobelts to MoO_2 Nanorods: Structure Transformation and Electrical Transport. *ACS Nano* **2009**, *3*, 478–482.
(41) Mai, L. Q.; Gao, Y.; Guan, J. G.; Hu, B.; Xu, L.; Jin, W. Formation and Lithiation of Ferroselite Nanoflowers as High-Energy Li-ion Battery Electrodes. *Int. J. Electrochem. Sci.* **2009**, *4*, 755–761.
(42) Delmas, C.; Brethes, S.; Menetrier, M. ω-$Li_3V_2O_5$-A New Electrode Material for Rechargeable Lithium Batteries. *J. Power Sources* **1991**, *34*, 113–118.
(43) Delmas, C.; Cognac-Auradou, H.; Cocciantelli, J. M.; Menetrier, M.; Doumerc, J. P. The $Li_xV_2O_5$ System: An Overview of The Structure Modifications Induced by The Lithium Intercalation. *Solid State Ionics* **1994**, *69*, 257–264.

DOI: 10.1021/nl103343w | *Nano Lett.* **2010,** *10,* 4750–-4755